PHYSICAL REVIEW D **78,** 063515 (2008)

Large curvature perturbations near horizon crossing in single-field inflation models

Edgar Bugaev* and Peter Klimai+

Institute for Nuclear Research, Russian Academy of Sciences, 60th October Anniversary Prospect 7a, 117312 Moscow, Russia

(Received 1 July 2008; published 10 September 2008)

We consider the examples of single-field inflation models predicting large amplitudes of the curvature perturbation power spectrum at relatively small scales. It is shown that in models with an inflationary potential of double-well type the peaks in the power spectrum, having, in maximum, the amplitude $\mathcal{P}_{\mathcal{R}} \sim 0.1$, can exist (if parameters of the potential are chosen appropriately). It is shown also that the spectrum amplitude of the same magnitude (at large k values) is predicted in the model with the running mass potential, if the positive running, n', exists and is about 0.005 at cosmological scales. Estimates of the quantum diffusion effects during inflation in models with the running mass potential are given.

DOI: 10.1103/PhysRevD.78.063515 PACS numbers: 98.80.Cq, 04.70.−s

I. INTRODUCTION

In the last few months several papers appeared [1–4] in which single-field inflation models predicting (potentially) large amplitudes of the curvature perturbations on relatively small scales are discussed. It is shown in [1] that a large class of such models exists, namely, the models with a potential of hill-top type (the idea of the hill-top inflation was proposed, to the author's knowledge, in the earlier work [5]). In such models, the potential can be of concave-downward form at cosmological scales (in accordance with data) and be much flatter at the end of inflation when small scales leave the horizon. Correspondingly, the amplitude of the perturbation power spectrum can be rather large. It is noticed in [1] that the running mass model, having the potential with the similar behavior, also can predict the large spectrum amplitude.

The authors of [2] discuss also more general scenarios of producing large amplitudes of perturbation spectrum. They show the limitedness of the standard procedure of the potential reconstruction which can easily miss the potentials leading to a large spectrum amplitude and to noticeable primordial black hole (PBH) production.

In the recent paper [3] it was shown that PBH production is possible in single-field models of two-stage type (''chaotic + new''). The idea was proposed ten years ago in [6]. The authors of [3] carried out the numerical calculation of the power spectrum using the Coleman-Weinberg (CW) potential.

In the present paper we continue a study of the problems discussed in the previous works [1–3]. We investigated thoroughly, as a particular example, the model of two-stage inflation with a potential of the double-well (DW) form, and showed that the characteristic features of the power spectrum in models of this type (such as an amplitude and a position of the peak, a degree of tuning of parameters of the potential) are very sensitive to an exact form of the potential. Further, we carried out the numerical calculation of the power spectrum in a running mass model and showed that the spectrum amplitude at small scales can be rather large. Our calculation differs from the previous one [7] in several aspects: we express the results through the values of parameters s, c, which are used nowadays and prove to be very convenient for a comparison with data; we studied, in detail, the difference in predictions of slow-roll and numerical approaches at high k-values; we exactly specified the value of the positive running, n', which corresponds to our spectrum prediction. In the final part of the work we investigated the quantum diffusion effects in a model with the running mass potential.

A plan of the paper is as follows. In the second section we study predictions of two-stage inflation models with DW and CW potentials, with accent on a mechanism of the formation of peaks in the power spectrum. In Sec. III all aspects connected with an obtaining of the predictions of running mass inflation models are discussed. In Sec. IV we present our main conclusions.

II. EXAMPLES OF THE POWER SPECTRUM WITH PEAKS

A. Double-well potential

This form of the inflaton potential having an unstable local maximum at the origin has been discussed many times in studies of eternal and new inflation. The main problem was to realize the initial condition for the new inflation when the system starts from a top of the hill. Ten years ago the model of ''chaotic new inflation'' has been proposed [6], in which the system climbs on the top during dynamical evolution of the inflaton field with initial conditions coinciding with those of chaotic inflation models. In the approach of [6] the inflation has two stages, chaotic and new, and during transition from the first stage to the second the slow-roll conditions break down (in general).

*bugaev@pcbai10.inr.ruhep.ru
+pklimai@gmail.com

The potential has two parameters:

$$V(\phi) = \frac{\lambda}{4}(\phi^2 - v^2)^2. \tag{1}$$

The inflaton starts with the rather high value of ϕ (we take $\phi_{\rm in} \sim 5m_{Pl}$) and rolls down to the origin. The parameter λ is fixed by a normalization of the power spectrum on experimental data, $\lambda \sim 10^{-13}$. The evolution of the system strongly depends on the value of v: if v is finely tuned, ϕ can spend some time near the origin, i.e. on the top, and then roll down to one of the two minima. In Figs. 1 and 2(a) the time evolution for the inflaton and the parameter ϵ for the definite values of the parameters λ, v are shown. One can see that, really, $\phi \approx 0$ at some period of time and, what is important, the slow-roll approximation is invalid ($\epsilon \sim 1$) just at the time of the transition from a rolling to a temporary stay at the top of the potential.

It is well known that in situations when there is a failure of the slow-roll evolution the perturbations on superhorizon scales can be amplified and specific features in the power spectrum can arise [8–12] (see also the recent paper [13]). In particular, in the earliest work where this problem was studied [8], the inflation potential with a sudden gradient discontinuity leading to the power spectrum of a steplike form was considered. All this means that the predictions of the slow-roll approximation which are based on the assumption that perturbations reach an asymptotic regime outside the horizon cannot be trusted.

The curvature perturbation on comoving hypersurfaces $\mathcal{R}_k$, as a function of the conformal time τ, is a solution of the differential equation (prime denotes the derivative over τ)

$$\mathcal{R}_k'' + 2\frac{z'}{z}\mathcal{R}_k' + k^2\mathcal{R}_k = 0, \tag{2}$$

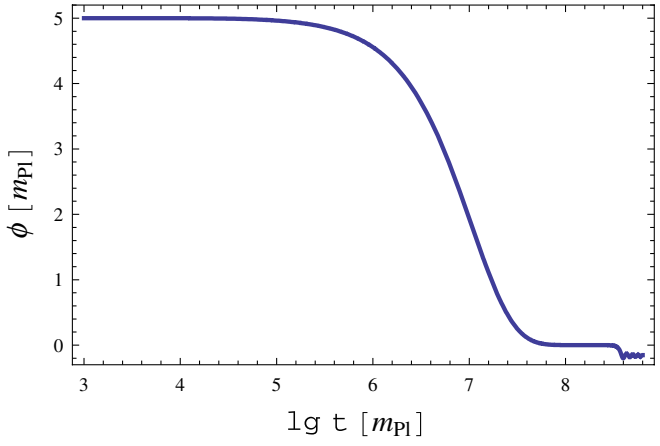

FIG. 1 (color online). The solution of the background equation for inflation with the double-well potential (1). The parameters of the potential are: $v = 0.162\,867\,48 m_{Pl}$, $\lambda = 1.7 \times 10^{-13}$.

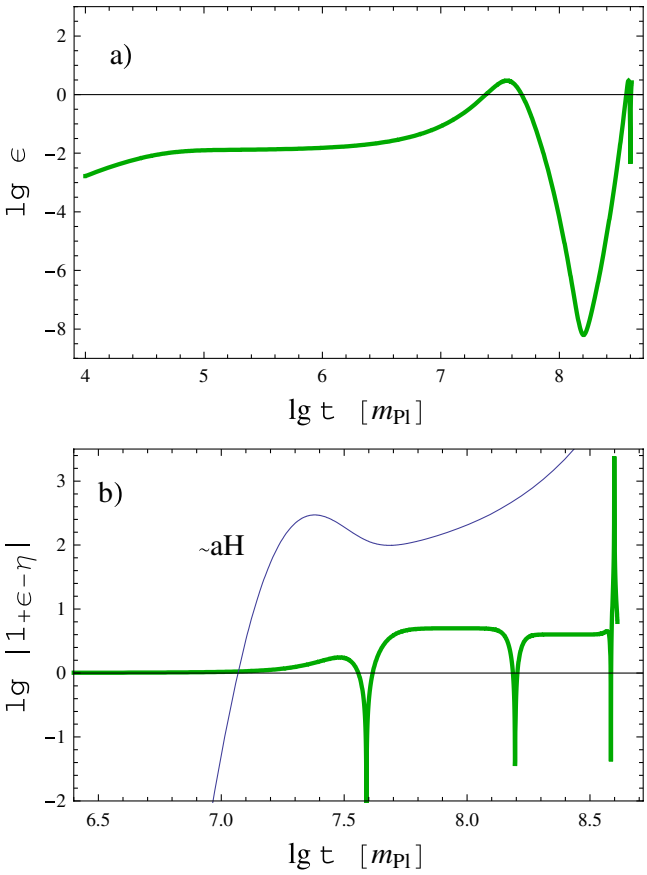

FIG. 2 (color online). The time dependence of the parameter ϵ and the combination $1 + \epsilon - \eta$ corresponding to the background field evolution shown in Fig. 1.

$$\frac{z'}{z} = aH(1 + \epsilon - \eta), \qquad z \equiv \frac{a\dot{\phi}}{H} \tag{3}$$

(ϕ is the inflaton field). The standard initial condition for this equation, corresponding to the Bunch-Davies [14] vacuum, is

$$u_k(\tau) = \frac{1}{\sqrt{2k}} e^{-ik\tau}, \qquad aH \ll k, \tag{4}$$

where $u = z\mathcal{R}$. The variable u had been introduced in [15–17].

The functions ϵ and η in Eq. (3) are the Hubble slow-roll parameters defined by the expressions [18]

$$\epsilon = -\frac{\dot{H}}{H^2} = \frac{4\pi}{m_{Pl}^2}\frac{\dot{\phi}^2}{H^2}, \qquad \eta = -\frac{\ddot{\phi}}{H\dot{\phi}}. \tag{5}$$

Outside the slow-roll limit these functions are not necessarily small.

It had been demonstrated in [11] that solutions of Eq. (2), at $k \ll aH$, i.e., outside the horizon, are well approximated by a constant if the coefficient of the friction term, z'/z, does not change sign near the horizon crossing. In the opposite case, if z'/z changes sign at some time, the

friction term becomes a negative driving term, and one can expect strong effects on modes which left the horizon near that time. In the present paper we study the corresponding features of the power spectrum, following closely the analysis of [11].

According to Eq. (3), z'/z is proportional to $1 + \epsilon - \eta$ and the comoving Hubble wave number aH. The time dependences of these functions are shown in Fig. 2(b). One can see that the interruption of inflation correlates with the change of the sign of $1 + \epsilon - \eta$.

The time evolution of curvature perturbations for several modes is shown in Fig. 3. It is clearly seen that the perturbations $\mathcal{R}_k$ for different modes freeze out at different amplitudes. The mode which crosses the horizon near the moment of time when the sign of $1 + \epsilon - \eta$ changes (i.e., near $t \approx 7.5 m_{Pl}$) freezes at maximum amplitude, due to the exponentially growing driving term in Eq. (2) (which is most effective just for this mode). It leads to the characteristic peak in the power spectrum $\mathcal{P}_\mathcal{R}(k)$,

$$\mathcal{P}_\mathcal{R}(k) = \frac{4\pi k^3}{(2\pi)^3} |\mathcal{R}_k|^2, \tag{6}$$

shown in Fig. 4.

The calculations of $\mathcal{R}_k$ (Fig. 3) are carried out up to the end of inflation, and the power spectrum in Fig. 4 also corresponds to this moment of time. We estimate approximately the reheat temperature in our case as $\sim(\lambda v^4)^{1/4} \sim 10^{14}$ GeV. The horizon mass at the beginning of the radiation era is

$$M_{hi} \sim 10^{17}\ \mathrm{g}\left(\frac{10^7\ \mathrm{GeV}}{T_{\mathrm{RH}}}\right)^2 \sim 10^3\ \mathrm{g}, \tag{7}$$

and the maximum wave number, which equals the Hubble radius at the end of inflation, is

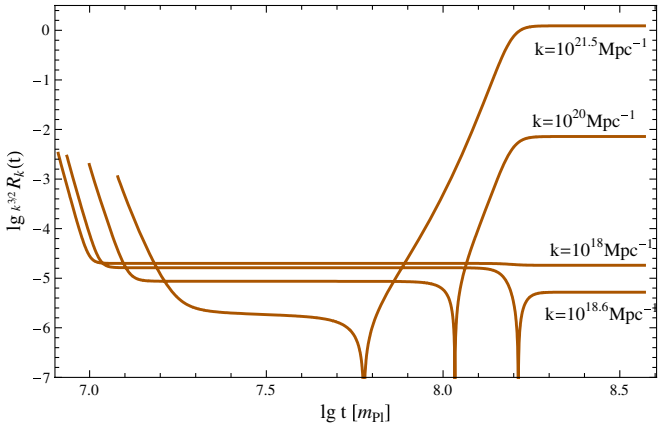

FIG. 3 (color online). A time evolution of the curvature perturbation $\mathcal{R}_k(t)$ for several different values of wave number k during inflation with the DW potential. The parameters of the potential are the same as in Fig. 1.

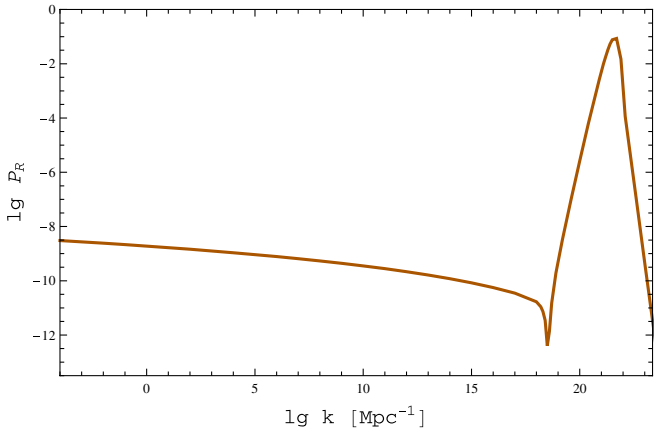

FIG. 4 (color online). The numerically calculated power spectrum $\mathcal{P}_\mathcal{R}(k)$ for the model with the potential (1). Parameters of the potential used in the calculation are the same as in Fig. 1.

$$k_{\mathrm{end}} = a_{\mathrm{eq}} H_{\mathrm{eq}} \left(\frac{M_{\mathrm{eq}}}{M_{hi}}\right)^{1/2} \sim 10^{23}\ \mathrm{Mpc}^{-1}. \tag{8}$$

In Fig. 5 we show the power spectrum calculated for two stages of its evolution: at the horizon exit (HE) and at the end of inflation (END). In the same figure the result of the calculation with a use of the slow-roll formulae is also shown. The peak of the HE curve at the region of large k is due to a failure (for $\mathcal{R}_k$) to reach the asymptotic limit. One can see also that the slow-roll approximation is too crude to describe perturbations at the end of inflation (thus our conclusion agrees with general statements of [11]).

B. Coleman-Weinberg potential

The Coleman-Weinberg potential has the form [19]:

$$V(\phi) = \frac{\lambda}{4}\phi^4\left(\ln\left|\frac{\phi}{v}\right| - \frac{1}{4}\right) + \frac{\lambda}{16}v^4. \tag{9}$$

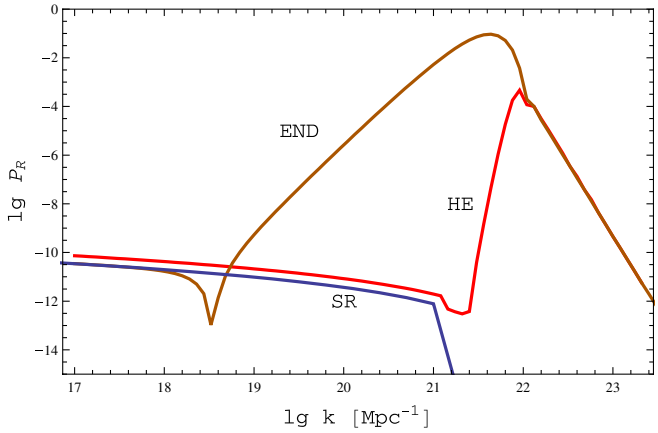

FIG. 5 (color online). The power spectrum $\mathcal{P}_\mathcal{R}(k)$ for the model with potential (1). END: $\mathcal{P}_\mathcal{R}(k)$ is calculated at the end of inflation; HE: $\mathcal{P}_\mathcal{R}(k)$ is calculated at the time of the horizon exit; SR: the slow-roll result.

It looks very similar to the previous one, but the important difference is its behavior near the origin. Namely, the CW potential behaves as $A + B\phi^4 \ln(\phi/v)$ near the origin, i.e., it is more flat near zero, in comparison with the DW potential. Therefore, it has more e-folds of "new inflation" [6] and, as a consequence, the peaks of the power spectrum (arising, as in the previous case, due to the temporary interruption of inflation) correspond to relatively smaller k values. Besides, at the beginning of new inflation when the very flat region of the potential near zero is crossed by ϕ, quantum fluctuations with a particle creation can be large (e.g., see below, Sec. III C) and must be taken into account.

In Fig. 6 two examples of the power spectrum calculations are shown for two different sets of parameter values. As before, the peaks are very distinct, although their amplitudes are smaller.

C. Possibilities of PBH production

One can see, in particular, from Fig. 4, that, in principle, the production of primordial black holes (about these objects, see the original works [20,21] and reviews [22,23]) can be rather large in single-field inflation models with potentials of double-well type. The main conclusion is that it requires a rather large fine-tuning of parameters of the potential. The characteristic PBH mass is estimated by

$$M_{\rm BH} \approx M_h = M_{hi}\left(\frac{k_{\rm end}}{k_{\rm peak}}\right)^2, \tag{10}$$

and in the case of the spectrum of Fig. 4, $M_{\rm BH} \sim 10^7$ g. In the CW case, Fig. 6, $M_{\rm BH} \sim 100 M_\odot$ for the left peak and $M_{\rm BH} \sim 10^{27}$ g for the right peak (but the amplitudes of the spectra are too small).

Recently, it has been shown [3] that inflation with the CW potential is capable to produce a significant number of PBHs: the parameter v can be chosen (by finest tuning) in such a way that the inflaton field makes several oscillations from one minimum to another before it climbs on the top and "new inflation" starts.

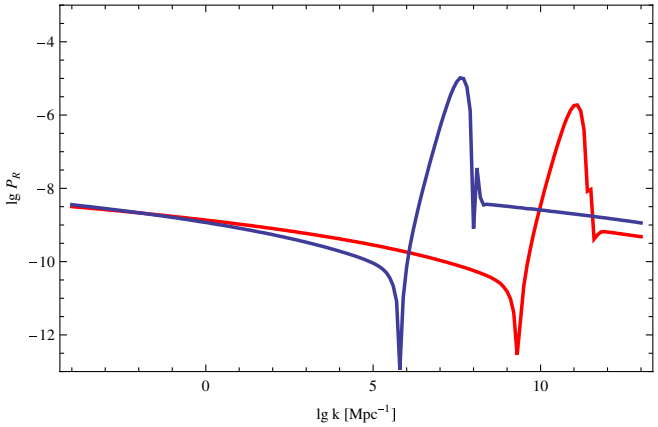

FIG. 6 (color online). The result for the power spectrum $\mathcal{P}_{\mathcal{R}}(k)$ calculation for the CW potential (9), for two sets of parameters. The left peak is for $v = 1.113 M_P$, $\lambda = 5.5 \times 10^{-13}$. For the right peak, $v = 1.112 M_P$, $\lambda = 2.4 \times 10^{-13}$.

In the present paper we do not consider possibilities of a constraining of the peak amplitudes, based, for example, on the effects of PBH evaporation in the early universe (see, e.g., [24]).

III. RUNNING MASS MODEL

A. Main assumptions and approximations

We consider in more detail a case of the running mass inflation model [25–31] which predicts a spectral index with rather strong scale dependence. The potential in this case takes into account quantum corrections in the context of softly broken global supersymmetry and is given by the formula

$$V = V_0 + \tfrac{1}{2} m^2 (\ln\phi)\phi^2. \tag{11}$$

The dependence of the inflaton mass on the renormalization scale ϕ is determined by the solution of the renormalization group equation (RGE).

(1) The inflationary potential in supergravity theory is of the order of $M_{\rm inf}^4$, where $M_{\rm inf}$ is the scale of supersymmetry breaking during inflation. In turn, the mass-squared of the inflaton (and any other scalar field) in supergravity has, in general, the order of the square of the Hubble expansion rate during inflation,

$$|m^2| \sim H_I^2 = \frac{V_0}{3M_P^2}. \tag{12}$$

We suppose, for simplicity (see [25,26,28,29]), that $M_{\rm inf} \sim M_{\rm s}$, where $M_{\rm s}$ is the scale of supersymmetry breaking in the vacuum,

$$M_{\rm s} \sim \sqrt{\tilde{m}_s M_P} \sim 10^{11}\ {\rm GeV} \sim 3 \times 10^{-8} M_P \tag{13}$$

($\tilde{m}_s$ is the scale of squarks and slepton masses, $\tilde{m}_s \sim$ 3 TeV). These assumptions give the scale of the inflationary potential:

$$V_0 \sim M_{\rm s}^4 \sim 10^{-30} M_P^4, \qquad H_I \approx 10^{-15} M_P. \tag{14}$$

(2) RGE for the inflaton mass is the following (we consider a model [28,29] of hybrid inflation using the softly broken SUSY with gauge group $SU(N)$ and small Yukawa coupling):

$$m^2(t) = m_0^2 - A\tilde{m}_0^2\left[1 - \frac{1}{(1+\tilde{\alpha}_0 t)^2}\right], \qquad t \equiv \ln\frac{\phi}{M_P}, \tag{15}$$

m_0^2 and $\tilde{m}_0^2$ are, correspondingly, the inflaton and gaugino masses at $\phi = M_P$,

$$\tilde{\alpha}_0 = \frac{B\alpha_0}{2\pi}, \tag{16}$$

α_0 is the gauge coupling constant, $\alpha_0 = g^2/4\pi$. A and B are positive numbers of order 1, which are different for different variants of the model, even if they are based on the same supersymmetric gauge group $SU(N)$ (it depends on a form of the superpotential, particle content of supermultiplets, etc). We use in the present paper the variant of [29] and, correspondingly, put everywhere below $A = 2$ and $B = N = 2$.

(3) A truncated Taylor expansion of the potential around the particular scale ϕ_0 (in our case, ϕ_0 is the inflaton value at the epoch of the horizon exit for the pivot scale $k_0 \approx 0.002h$ Mpc^{-1}) is

$$V(\phi) = V_0 + \frac{\phi^2}{2}\left[m^2(\ln(\phi_0)) - c\frac{V_0}{M_P^2}\ln\frac{\phi}{\phi_0} + \ldots\right]. \tag{17}$$

Here, constant c is defined by the equation

$$c\frac{V_0}{M_P^2} = -\frac{dm^2}{d\ln\phi}\bigg|_{\phi=\phi_0}. \tag{18}$$

In turn, a Taylor expansion of Eq. (15) up to linear terms gives ($t_0 = \ln\frac{\phi_0}{M_P}$):

$$m^2(t) = m^2(t_0) - 4\tilde{m}_0^2\frac{\tilde{\alpha}_0}{(1+\tilde{\alpha}_0 t_0)^3}\ln\frac{\phi}{\phi_0}. \tag{19}$$

From Eqs. (18) and (19) we obtain the expression for the constant c,

$$c\frac{V_0}{M_P^2} = 4\tilde{m}_0^2\frac{\tilde{\alpha}_0}{(1+\tilde{\alpha}_0 t_0)^3}. \tag{20}$$

If $|m_0^2| \sim \tilde{m}_0^2 \approx H_I^2$, then

$$c = \frac{4}{3}\frac{\tilde{\alpha}_0}{(1+\tilde{\alpha}_0 t_0)^3}. \tag{21}$$

It appears [see Fig. 7(b)] that in our example $\phi_0 \sim 10^{-10}M_P$, so, $t_0 \sim \ln 10^{-10} \sim (-23)$. Assuming that $\alpha_0 \sim 1/24$ (as in SUSY-grand unified theory (GUT) models), one has $\tilde{\alpha}_0 \sim \frac{2}{2\pi}\frac{1}{24}$. In such a case, $c \sim 4\tilde{\alpha}_0 \sim 0.06$.

If we would keep terms of higher order in $t - t_0 = \ln\frac{\phi}{\phi_0}$ in the Taylor expansion of $m^2(t)$ in Eq. (19) we would see that the real expansion parameter is $\tilde{\alpha}_0\ln\frac{\phi}{\phi_0}$ rather than $\ln\frac{\phi}{\phi_0}$. The smallest value of ϕ, $\phi_{\rm end}$, in our case is $\sim 10^{-16}M_P$ [see Fig. 7(b)]. Even for such a value of $\phi_{\rm end}$, the expansion parameter is rather small,

$$\tilde{\alpha}_0\ln\frac{\phi_{\rm end}}{\phi_0} \sim \tilde{\alpha}_0\ln 10^{-6} \sim (-0.1). \tag{22}$$

Having this in mind, we will use the linear approximation for the inflaton mass [Eq. (19)] in the entire region of inflaton field values exploited in the present paper.

Following the previous papers, we introduce also another parameter,

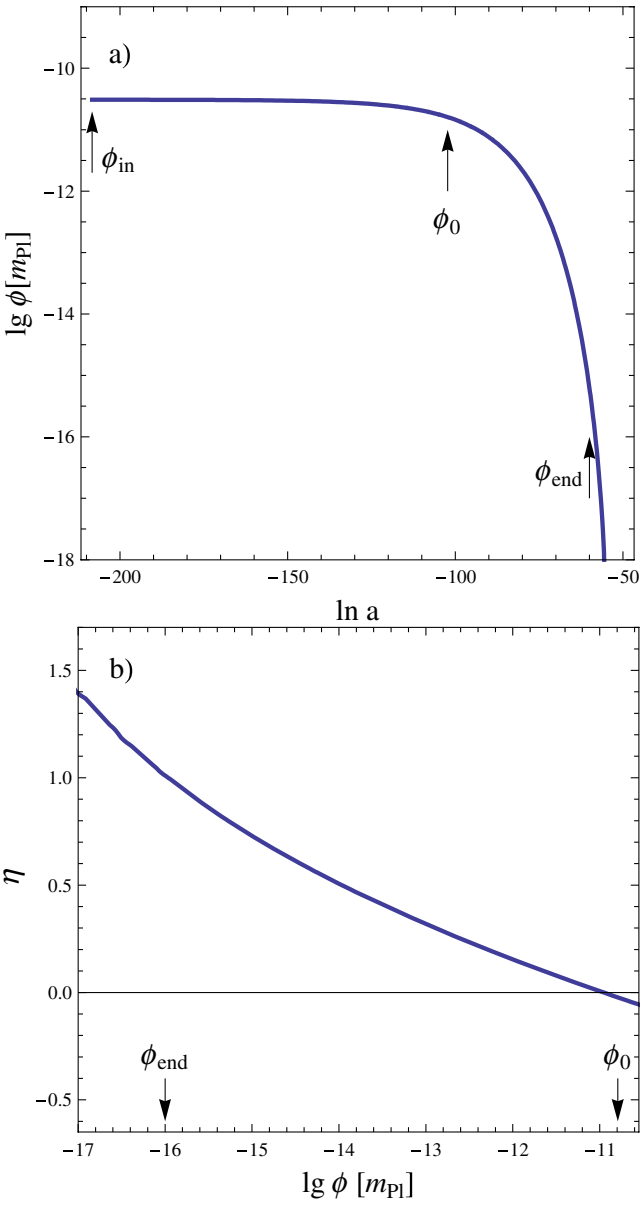

FIG. 7 (color online). (a) Evolution of the inflaton field $\phi(\ln a)$ in the running mass model. (b) The dependence of the parameter η on a value of the field ϕ. For both plots, $H_I = 10^{-15}M_P$, $c = 0.062$, $s = 0.040$.

$$s = c \ln\left(\frac{\phi_*}{\phi_0}\right), \tag{23}$$

where ϕ_* is the inflaton value corresponding to a maximum of the potential. This parameter connects the field value ϕ_0 with the Hubble parameter during inflation and with the normalization of the cosmic microwave background (CMB) power spectrum:

$$\phi_0 s = \frac{H_I}{2\pi \mathcal{P}_{\mathcal{R}}^{1/2}(k_0)}. \tag{24}$$

(4) The minimum value of the inflaton field which corresponds to the end of inflation can be determined from the approximate equation [29]

$$\eta = M_P^2 \frac{V''}{V} \cong \frac{M_P^2}{V_0} m^2 = 1. \tag{25}$$

Using RGE, one obtains from this formula the relation

$$\frac{M_P^2}{V_0}\left(m_0^2 - A\tilde{m}_0^2 + \frac{A\tilde{m}_0^2}{(1+\tilde{\alpha}_0 t)^2}\right) = 1. \tag{26}$$

Substituting here $A = 2$, $\tilde{m}_0^2 = |m_0^2| = V_0/3M_P^2$, one has finally the approximate expression for $\phi_{\rm end}$,

$$\phi_{\rm end} = M_P \exp\left[-\frac{1}{\tilde{\alpha}_0}\left(1 - \frac{1}{\sqrt{3}}\right)\right], \tag{27}$$

which shows that the minimum field value is very sensitive to the value of the model parameter $\tilde{\alpha}_0$ and, in our case, does not depend on V_0. More exactly, the condition $\eta = 1$ means the end of the *slow-roll part* of inflation. We suppose, as usual (see, e.g. [25,26]) that in reality inflation ends by a hybrid mechanism, and the critical value of the inflaton field, $\phi_{\rm cr}$, is determined by the value of the Yukawa coupling λ (in spite of the inequality $\lambda^2 \ll \alpha$). One can check [29] that the value of λ can always be chosen such that $\phi_{\rm cr} < \phi_{\rm end}$ and slow-roll ends before the reaching of $\phi_{\rm cr}$.

One should note that the accuracy of the approximate formula (27) is not very good. Luckily, in the approach based on the numerical calculation of the power spectrum there is no need to use it, because the value of $\phi_{\rm end}$ appears in a course of the calculation [Fig. 7(b)].

B. Power spectrum of curvature perturbations

An analysis of CMB anisotropy data [32,33], including other types of observation [34], leads to the following main qualitative conclusions:

(i) the power spectrum of scalar curvature perturbations is red, i.e., the spectral index is negative,

$$n_0 = 0.97 \pm 0.01; \tag{28}$$

(ii) observations are consistent, or, at least, are not in contradiction with the small positive running of the spectral index, $n_0' < 0.01$;

(iii) the contribution of tensor perturbations in the value of the spectral index is small ($\lesssim 10^{-2}$) and, as a result, $n \approx 1 + 2\eta$; it means that η is negative, and the potential must be concave-downward (i.e., of hill-top type), while cosmological scales cross the horizon during inflation [1].

One should note that, strictly speaking, the conclusion (iii) is not grounded firmly enough. According to the recent analysis [35], the present data still admit any sign of η and V''.

These conclusions constrain the possible values of the parameters s and c. Approximately, for the cosmological scale, one has

$$n_0 - 1 \approx 2(s - c), \qquad n_0' \approx 2sc. \tag{29}$$

From the conclusion (iii) it follows that $c > 0$ (it is consistent with Eq. (24)), from the positivity of n_0' (the conclusion (ii)) it follows that $s > 0$. At last, the conclusion (i) leads to the inequality $s < c$.

We choose for the power spectrum calculation the following values:

$$c = 0.062, \qquad s = 0.040. \tag{30}$$

These numbers correspond, at cosmological scales, to the following values of slow-roll parameters:

$$\epsilon \approx \frac{s\phi_0^2}{M_P^2} \sim 10^{-21}; \qquad \eta \approx s - c \sim (-0.02), \tag{31}$$

that seems to be consistent with the present data [4].

To check the validity of the slow-roll approximation, we calculate the spectrum by the three ways: (i) using the approximate analytic slow-roll formula

$$\frac{\mathcal{P}_{\mathcal{R}}(k)}{\mathcal{P}_{\mathcal{R}}(k_0)} = \exp\left[\frac{2s}{c}(e^{c\Delta N(k)} - 1) - 2c\Delta N(k)\right] \tag{32}$$

($\Delta N(k) \equiv \ln(k/k_0)$; this expression is easily derived from the simplest slow-roll prediction

$$\mathcal{P}_{\mathcal{R}}(k) = \left.\frac{H^2}{\pi\epsilon m_{Pl}^2}\right|_{aH=k}, \tag{33}$$

which gives the power spectrum to leading order in the slow-roll approximation [36]); (ii) using the Stewart-Lyth approximation [37], which is valid to first order in the slow-roll approximation,

$$\mathcal{P}_{\mathcal{R}}^{1/2}(k) = [1 - (2C+1)\epsilon + C\eta]\frac{1}{2\pi}\left.\frac{H^2}{|\dot{\phi}|}\right|_{aH=k}, \tag{34}$$

$$C \approx -0.73;$$

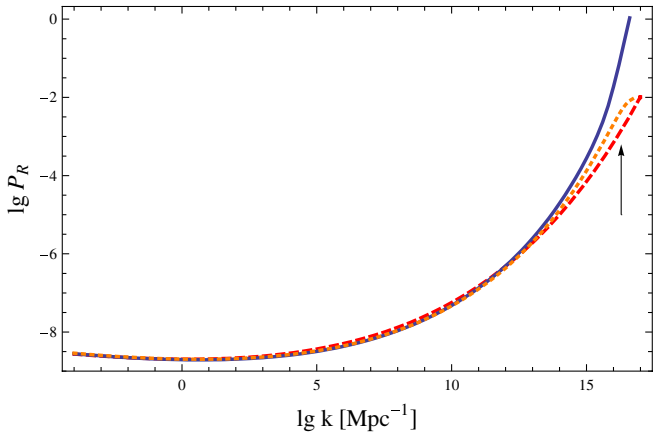

FIG. 8 (color online). Power spectrum $\mathcal{P}_{\mathcal{R}}(k)$ in the running mass model, calculated numerically (solid line), by the approximate analytic formula (32) (long-dashed line) and using the Stewart-Lyth extended slow-roll approximation (short-dashed line). The parameters of the potential are the same as used in Fig. 7. The arrow shows the value of $k_{\rm end}$.

(iii) by numerical integration of the differential equation for $\mathcal{R}_k$, Eq. (2).

The results of the calculations are presented in Figs. 7–9. Figure 7 shows the evolution of the inflaton field ϕ with the scale factor and a growth of the slow-roll parameter η with a decrease of ϕ from ϕ_0 to $\phi_{\rm end}$. The power spectrum is shown in Fig. 8 for a broad interval of comoving wave numbers. It is clearly seen that near the end of inflation, when

$$\begin{aligned} &\phi \sim 10^{-16} M_P, \\ &k \sim k_{\rm end} = a_{\rm end} H_{\rm end} = 3 \times 10^{16}\ {\rm Mpc}^{-1}, \end{aligned} \tag{35}$$

the slow-roll formulae are inaccurate: they strongly underestimate values of $\mathcal{P}_{\mathcal{R}}$. To illustrate this point more clearly,

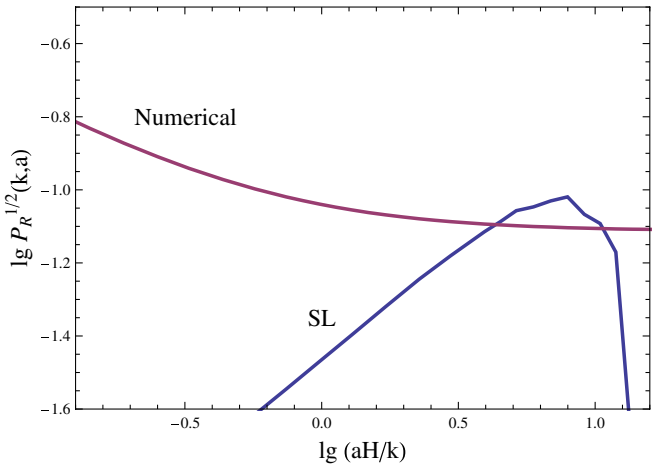

FIG. 9 (color online). Dependence of $\mathcal{P}_{\mathcal{R}}(k, a)$ calculated numerically and $\mathcal{P}_{\mathcal{R}}$ from the Stewart-Lyth formula. The comoving wave number for this figure is $k = 10^{15.8}$ Mpc^{-1}.

at the next figure we show the comparison of two curves: aH-dependence of the spectrum calculated numerically for a definite value of k, $k = 10^{15.8}$ Mpc^{-1}, and aH-dependence of the Stewart-Lyth spectrum. It is seen that the numerical spectrum at the moment of crossing horizon (when $aH = k$) is already almost asymptotical and its value distinctly exceeds the corresponding value predicted by the Stewart-Lyth formula.

C. Quantum diffusion effects

We calculated the curvature perturbations in terms of the classical trajectories of a scalar field associating, in particular, points in a field space with definite numbers of e-folds from the end of inflation. This description becomes incorrect if the quantum diffusion destroys the classical evolution of the field. In this case we should use the methods of stochastic inflation. The latter approach operates with the coarse-grained field, which is defined to be the spatial average of the field ϕ over a physical volume with size larger than the Hubble radius H^{-1}.

In the slow-roll approximation, the evolution of the coarse-grained field φ is governed by the first order Langevin-like equation [38–41]

$$\dot{\varphi} + \frac{1}{3H} V'(\varphi) = \frac{H^{3/2}}{2\pi} \xi(t), \tag{36}$$

$$\langle \xi(t) \rangle = 0, \qquad \langle \xi(t) \xi(t') \rangle = \delta(t - t'). \tag{37}$$

Here, $\xi(t)$ is a random noise field and angular brackets mean ensemble average. The term $\frac{1}{3H} V'(\varphi)$ describes the deterministic evolution of the field φ, in the absence of the noise term $\frac{H^{3/2}}{2\pi} \xi(t)$. The solution of Eq. (36), in the absence of the noise term, is the deterministic slow-roll trajectory $\varphi_{\rm sr}(t)$. Going to finite time differences, the coefficient $\frac{H^{3/2}}{2\pi}$ can be rewritten as $\sqrt{\frac{H^3}{4\pi^2 \Delta t}}$, and the evolution of φ on time scales $\Delta t \geq H^{-1}$ can be described by a finite-difference form of Eq. (36),

$$\varphi(t + \Delta t) - \varphi(t) = -\frac{1}{3H} V'(\varphi) \Delta t + \frac{1}{2\pi} \sqrt{H^3 \Delta t}\, \xi(t). \tag{38}$$

The condition for the deterministic evolution is (see, e.g., [42])

$$\frac{1}{3H} |V'(\varphi)| \Delta t \gg \frac{1}{2\pi} \sqrt{H^3 \Delta t}, \qquad \Delta t = H^{-1}. \tag{39}$$

Using the slow-roll connection between V and H, one obtains

$$|V'(\varphi)| \gg \frac{3}{2\pi} H^3 = \frac{1}{2\pi\sqrt{3}} V^{3/2}(\varphi). \tag{40}$$

In the approach of [43] the coarse-grained field is considered as a perturbation of the classical solution $\varphi_{\rm cl}$ (which is the solution of the Langevin equation without

the noise),

$$\varphi(t) = \varphi_{\rm cl}(t) + \delta\varphi_1(t) + \delta\varphi_2(t) + \ldots \qquad (41)$$

Here, the term $\delta\varphi_i(t)$ depends on the noise at the power i. It is assumed that the Hubble parameter in the Langevin equation depends only on the coarse-grained field φ,

$$H^2(\varphi) = \frac{1}{3M_P^2} V(\varphi). \qquad (42)$$

Correspondingly, the Hubble parameter can be expanded perturbatively,

$$H(\varphi) = H_{\rm cl} + H'_{\rm cl}(\delta\varphi_1 + \delta\varphi_2) + \frac{H''_{\rm cl}}{2}\delta\varphi_1^2 + \ldots, \qquad (43)$$

$$H_{\rm cl} = H(\varphi_{\rm cl}) = \sqrt{\frac{V(\varphi_{\rm cl})}{3M_P^2}}. \qquad (44)$$

This approach permits to calculate the mean value of the total number of e-folds, $\langle N\rangle$, and to compare it with the corresponding "classical" number,

$$N_T^{\rm cl} = -\frac{1}{2M_P^2}\int_{\varphi_{\rm in}}^{\varphi_{\rm end}} d\varphi_{\rm cl}\frac{H_{\rm cl}}{H'_{\rm cl}} = \frac{1}{M_P^2}\int_{\varphi_{\rm end}}^{\varphi_{\rm in}} d\varphi_{\rm cl}\left(\frac{V}{V'}\right); \qquad (45)$$

$$\delta N_T = \langle N_T\rangle - N_T^{\rm cl} = -\frac{1}{2M_P^2}\int_{\varphi_{\rm in}}^{\varphi_{\rm end}}\left[\langle\delta\varphi_2\rangle + \frac{H''_{\rm cl}}{2H'_{\rm cl}}\langle\delta\varphi_1^2\rangle\right]d\varphi_{\rm cl}. \qquad (46)$$

Besides, one can calculate the mean value of the Gaussian probability distribution function for the coarse-grained field and to see how it behaves as a function of the current field value.

The interval of inflaton field values for which the inequality (40) holds and, therefore, the deterministic evolution dominates, is shown in Fig. 10(a) and 10(b). The variable x in Fig. 10(b) is defined by the relation

$$\frac{\varphi_{\rm in}}{\varphi_*} = 1 - 10^{-x} \qquad (47)$$

(φ_* is, as before, the point of a maximum of the potential $V(\varphi)$). It is seen from the figure that the constraints on the inflaton field following from the condition (40) are not too severe,

$$3\times 10^{-19} M_P \lesssim \varphi \lesssim \varphi_* - 10^{-7}\varphi_*. \qquad (48)$$

An accuracy of the perturbative expansion (41) for the monomial potential of stochastic inflation models was studied in [44]. Here we study this accuracy for the running mass potential, using the parameters V_0, s, c, $\varphi_{\rm end}$ introduced above. The results of the calculation of $\langle\delta\varphi_1^2\rangle$ and $\langle\delta\varphi_2\rangle$ are shown in Fig. 11. As one can see, the perturbative expansion is good if the starting value of the inflaton field, $\varphi_{\rm in}$, is chosen to be not too close to the value of φ at the maximum of the potential. More exactly, the parameter x, defined in Eq. (47), must be smaller than $4 \div 4.5$. The starting value $\varphi_{\rm in}$ corresponds to a beginning of the evolution, i.e., $\delta\varphi_1(t_{\rm in}) = \delta\varphi_2(t_{\rm in}) = 0$.

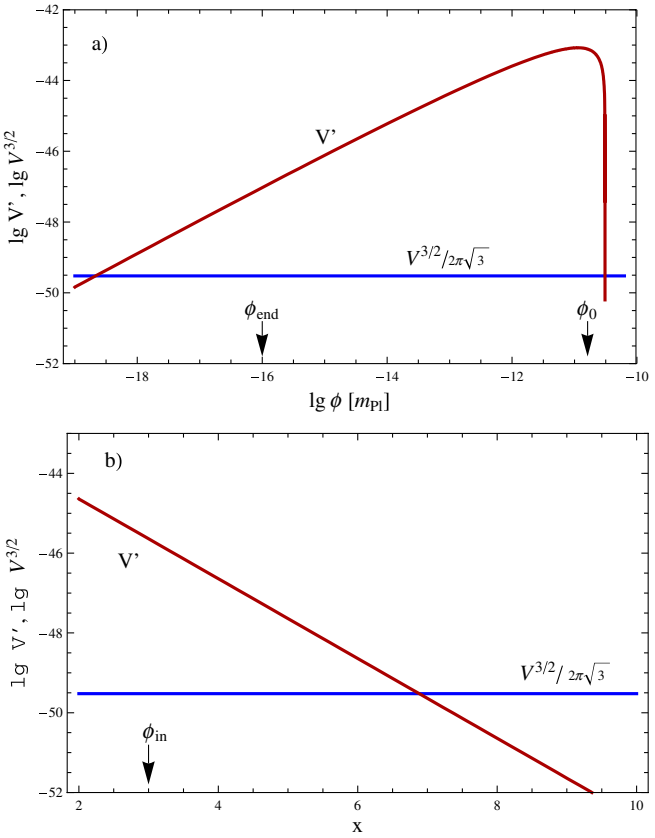

FIG. 10 (color online). (a) Comparison of V' and $V^{3/2}$ for the running mass model [see Eq. (40)]. (b) The same figure in a different scale: variable x is connected to the field value by the relation $\varphi = (1 - 10^{-x})\varphi_*$.

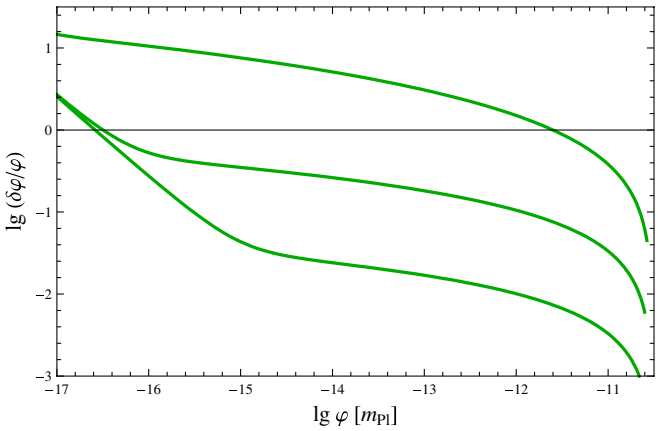

FIG. 11 (color online). The result for the calculation of $\delta\varphi/\varphi$ for different values of $\varphi_{\rm in} = \varphi_*(1 - 10^{-x})$. From bottom to top, x equals 3, 4, 5. Here, $\delta\varphi \equiv \sqrt{\langle\delta\varphi_1^2\rangle} + \langle\delta\varphi_2\rangle$.

If the evolution is deterministic, the correction to a classical e-fold number $N_T^{\rm cl}$, given by Eq. (46), is small. To estimate analytically the upper limit for this correction, we used the analytic expressions for $\langle\delta\varphi_1^2\rangle$ and $\langle\delta\varphi_2\rangle$ derived in [43], keeping in them leading terms only. According to these expressions, the following inequalities hold:

$$\langle\delta\varphi_2\rangle < \left(\frac{V_0}{M_P}\right)^4\left(\frac{M_P}{\varphi_{\rm in}}\right)^2\frac{1}{\ln^2\frac{\varphi_{\rm in}}{\varphi_*}}\frac{\varphi}{M_P} \lesssim 10^{-10+2x}\varphi, \quad (49)$$

$$\langle\delta\varphi_1^2\rangle < \left(\frac{V_0}{M_P}\right)^4\frac{1}{\ln^2\frac{\varphi_{\rm in}}{\varphi_*}} \sim 10^{-30+2x}M_P^2. \quad (50)$$

Using these upper limits, one can estimate the corresponding upper limits of two integrals in the expression for δN_T (46). The result is the following:

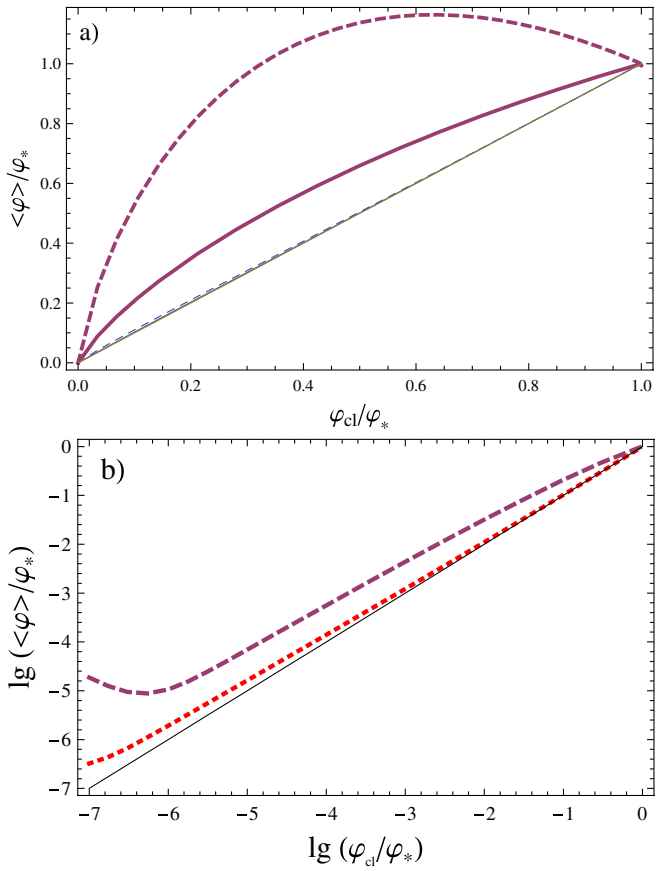

FIG. 12 (color online). Calculation of stochastic effects for various values of initial field $\varphi_{\rm in}$. (a) Thin dashed curve: $\varphi_{\rm in} = (1 - 1.5\times10^{-5})\varphi_*$, no volume effects included; thick dashed curve: $\varphi_{\rm in} = (1 - 1.5\times10^{-5})\varphi_*$, volume effects included; solid thick curve: $\varphi_{\rm in} = (1 - 3\times10^{-5})\varphi_*$, volume effects included. (b) Thick long-dashed and thick short-dashed curves correspond to the cases with and without the inclusion of volume effects, respectively, for $\varphi_{\rm in} = (1 - 3\times10^{-5})\varphi_*$.

$$\frac{1}{M_P^2}\int_{\varphi_{\rm end}}^{\varphi_{\rm in}}\langle\delta\varphi_2\rangle d\varphi_{\rm cl} < 10^{-30+2x}; \quad (51)$$

$$\frac{1}{M_P^2}\int_{\varphi_{\rm end}}^{\varphi_{\rm in}}\frac{\langle\delta\varphi_1^2\rangle H''_{\rm cl}}{H'_{\rm cl}}d\varphi_{\rm cl} < 10^{-30+3x}. \quad (52)$$

It is clear from the inequalities (52) that the quantum correction to e-fold number, δN_T, is quantitatively small even if the value of x is as large as 10. But only if $x < 4 \div 4.5$, and the perturbative expansion, Eq. (41), is valid, one really can be sure that

$$\delta N_T \ll N_T^{\rm cl}, \quad (53)$$

and the evolution is deterministic.

However, this analysis is still not complete: one must check also the position of the mean value of the probability distribution function for the coarse-grained field [43]. The calculation, with taking into account the volume effects, leads to the results shown in Fig. 12(a) and 12(b). It is seen from the figure that in this case also, as in the calculation of the e-fold number correction, the correct choice of the initial condition plays a decisive role: there are no effects of a "walk" of the mean value around the maximum of the potential (such effects were noticed in [43]) if evolution starts from the point which is far enough from the maximum ($x \lesssim 4.5$). Of course, the realization of the initial condition of this kind is, in itself, a problem. Supposedly, it could be provided by the previous history of eternal inflation [25,26].

IV. CONCLUSIONS

(1) It is shown, by numerical methods, that in the single-field inflationary model with a simple double-well potential the parameter values of this potential can be chosen in such a way that the power spectrum of curvature perturbations $\mathcal{P}_\mathcal{R}(k)$ has a huge peak (with amplitude $\sim$0.1) at large k (and the right normalization and monotonic behavior at cosmological scales). The peak arises due to temporary interruption of the slow-roll near points of the minimum of the potential, $\pm v$. The corresponding mass of PBHs produced in the early universe in a case of the realization of such a power spectrum is about 10^7 g.
The analogous behavior of the power spectrum was obtained by the authors of [3] in a model with CW potential. There are some important differences in the results of [3] and ours, in the peak amplitude and PBH mass, connected, in particular, with a large flatness near the origin in a case of the CW potential.

(2) It is shown that the inflation model with running mass potential predicts a rather large amplitude of the power spectrum of curvature perturbations (~ 0.1) at k values $\sim10^{16}$ Mpc^{-1}. For such a pre-

diction, a very small positive spectral index running at cosmological scales is necessary, $n' \sim 0.005$, as well as a small negative value for the slow-roll parameter η (≈ -0.02). Both these numbers do not contradict with the data. It is shown also that for obtaining the correct quantitative results for the power spectrum at largest k values a use of numerical methods is required because, in general, slow-roll formulas are not accurate enough at the end of inflation, where $\eta \approx 1$.

(3) Quantum diffusion effects in a model with the running mass potential are studied in detail. It is shown that inflationary evolution of the universe in a model with a scalar field and the running mass potential can be described by the classic deterministic equations, and for a possibility of such a description the correct choice of the initial conditions is crucial. Concretely, an initial value of the inflaton field (at the beginning of the evolution) should not be too close to a point of the maximum of the potential. If this condition is satisfied, the quantum corrections to a total e-fold number and to a position of the mean value of the probability distribution function are small.

ACKNOWLEDGMENTS

The authors are grateful to Professor A. A. Starobinsky for useful remarks. The work was supported by the Russian Foundation for Basic Research (Grant No. 06-02-16135).

[1] K. Kohri, C.-M. Lin, and D. H. Lyth, J. Cosmol. Astropart. Phys. 12 (2007) 004.
[2] K. Kohri, D. H. Lyth, and A. Melchiorri, J. Cosmol. Astropart. Phys. 04 (2008) 038.
[3] R. Saito, J. Yokoyama, and R. Nagata, J. Cosmol. Astropart. Phys. 06 (2008) 024.
[4] H. V. Peiris and R. Easther, arXiv:0805.2154.
[5] L. Boubekeur and D. H. Lyth, J. Cosmol. Astropart. Phys. 07 (2005) 010.
[6] J. Yokoyama, Phys. Rev. D **58**, 083510 (1998).
[7] S. M. Leach, I. J. Grivell, and A. R. Liddle, Phys. Rev. D **62**, 043516 (2000).
[8] A. A. Starobinsky, JETP Lett. **55**, 489 (1992).
[9] P. Ivanov, P. Naselsky, and I. Novikov, Phys. Rev. D **50**, 7173 (1994).
[10] J. S. Bullock and J. R. Primack, Phys. Rev. D **55**, 7423 (1997).
[11] S. M. Leach and A. R. Liddle, Phys. Rev. D **63**, 043508 (2001).
[12] S. M. Leach, M. Sasaki, D. Wands, and A. R. Liddle, Phys. Rev. D **64**, 023512 (2001).
[13] R. K. Jain, P. Chingangbam, and L. Sriramkumar, J. Cosmol. Astropart. Phys. 10 (2007) 003.
[14] N. D. Birrell and P. C. W. Davies, *Quantum Fields In Curved Space* (Cambridge University Press, Cambridge, England, 1982), p. 340.
[15] V. N. Lukash, JETP Lett. **31**, 596 (1980); Sov. Phys. JETP **52**, 807 (1980).
[16] V. F. Mukhanov, JETP Lett. **41**, 493 (1985); Sov. Phys. JETP **67**, 1297 (1988).
[17] M. Sasaki, Prog. Theor. Phys. **76**, 1036 (1986).
[18] A. R. Liddle, P. Parsons, and J. D. Barrow, Phys. Rev. D **50**, 7222 (1994).
[19] S. R. Coleman and E. Weinberg, Phys. Rev. D **7**, 1888 (1973).
[20] Y. B. Zeldovich and I. D. Novikov, Sov. Astron. **10**, 602 (1967).
[21] S. Hawking, Mon. Not. R. Astron. Soc. **152**, 75 (1971).
[22] B. J. Carr, arXiv:astro-ph/0511743.
[23] M. Y. Khlopov, arXiv:0801.0116.
[24] E. Bugaev and P. Klimai, arXiv:astro-ph/0612659.
[25] E. D. Stewart, Phys. Lett. B **391**, 34 (1997).
[26] E. D. Stewart, Phys. Rev. D **56**, 2019 (1997).
[27] L. Covi and D. H. Lyth, Phys. Rev. D **59**, 063515 (1999).
[28] L. Covi, D. H. Lyth, and L. Roszkowski, Phys. Rev. D **60**, 023509 (1999).
[29] L. Covi, Phys. Rev. D **60**, 023513 (1999).
[30] G. German, G. G. Ross, and S. Sarkar, Phys. Lett. B **469**, 46 (1999).
[31] L. Covi, D. H. Lyth, A. Melchiorri, and C. J. Odman, Phys. Rev. D **70**, 123521 (2004).
[32] D. N. Spergel *et al.* (WMAP Collaboration), Astrophys. J. Suppl. Ser. **170**, 377 (2007).
[33] J. Dunkley *et al.* (WMAP Collaboration), arXiv:0803.0586.
[34] J. Lesgourgues, M. Viel, M. G. Haehnelt, and R. Massey, J. Cosmol. Astropart. Phys. 11 (2007) 008.
[35] J. Lesgourgues, A. A. Starobinsky, and W. Valkenburg, J. Cosmol. Astropart. Phys. 01 (2008) 010.
[36] A. R. Liddle and D. H. Lyth, Phys. Rep. **231**, 1 (1993).
[37] E. D. Stewart and D. H. Lyth, Phys. Lett. B **302**, 171 (1993).
[38] A. A. Starobinsky, Phys. Lett. B **117**, 175 (1982).
[39] A. A. Starobinsky, in: *Field Theory, Quantum Gravity and Strings*, edited by H. J. de Vega and N. Sanchez, Lect. Notes in Physics Vol. 246 (Springer-Verlag, Berlin, 1986), p. 107.
[40] A. Vilenkin, Phys. Rev. D **27**, 2848 (1983); Nucl. Phys. **B226**, 527 (1983).
[41] A. D. Linde, Phys. Lett. B **175**, 395 (1986).
[42] S. Winitzki, Lect. Notes Phys. **738**, 157 (2008).
[43] J. Martin and M. Musso, Phys. Rev. D **73**, 043516 (2006).
[44] J. Martin and M. Musso, Phys. Rev. D **73**, 043517 (2006).